



Article

Multi-Temporal Analysis of the Impact of Summer Forest Dynamics on Urban Heat Island Effect in Yan'an City

Xinyi Wang, Yuan Chen, Zhichao Wang, Bo Xu and Zhongke Feng *

Precision Forestry Key Laboratory of Beijing, Beijing Forestry University, Beijing 100083, China;
shangdaoyizi@bjfu.edu.cn (X.W.); chenyuan5671@bjfu.edu.cn (Y.C.); zhichao@bjfu.edu.cn (Z.W.);
justinxubo@bjfu.edu.cn (B.X.)

* Correspondence: zhongkefeng@bjfu.edu.cn

Abstract: In this study, MODIS land products and China land cover datasets were used to extract normalized difference vegetation index, land surface temperature, and vegetation cover type in Yan'an City during the summers of 2017–2022. On this basis, analysis of spatial change and correlation were carried out as a way to study the mitigation effect on urban heat islands in Yan'an City with forest. The study showed that: (1) The coverage of normalized difference vegetation index over 0.4 in summer in Yan'an City increased from 59.38% to 69.12%, and the vegetation showed good growth conditions. It has a spatial distribution pattern of more in the south and less in the north. (2) The proportion of the urban heat island in Yan'an City increased from 15.51% to 16.86%. Urban heat island intensity fluctuated year by year, with the maximum urban heat island intensity of 6.26 °C appearing in 2019. It has a spatial distribution pattern of less in the south and less in the north. The transition rate of temperature field grade from low to high is 73.32%, and the transition rate to low is only 0.31%. (3) There is a negative correlation between land surface temperature and normalized difference vegetation index in Yan'an City. Vegetation has a mitigating effect on the UHI and the best cooling effect among the vegetation is shown by forest. The cooling effect of forest in Yan'an City is attenuated by an increase in distance, and the effective range is greater than 1000 m. In this study, the regulation effect of forest on the urban heat island was obtained by digging deeper into the intrinsic connection between spatial change in vegetation cover and land surface temperature change in Yan'an City. It provides an important reference for the formulation of meteorological protection policy as well as the promotion of sustainable development of the urban ecological environment and is of guiding significance for future urban planning and ecological construction.



Citation: Wang, X.; Chen, Y.; Wang, Z.; Xu, B.; Feng, Z. Multi-Temporal Analysis of the Impact of Summer Forest Dynamics on Urban Heat Island Effect in Yan'an City. *Sustainability* **2024**, *16*, 3473.
<https://doi.org/10.3390/su16083473>

Academic Editors: Monica Salvia and Attila Buzási

Received: 18 March 2024

Revised: 10 April 2024

Accepted: 19 April 2024

Published: 21 April 2024



Copyright: © 2024 by the authors. Licensee MDPI, Basel, Switzerland. This article is an open access article distributed under the terms and conditions of the Creative Commons Attribution (CC BY) license (<https://creativecommons.org/licenses/by/4.0/>).

1. Introduction

The urban heat island (UHI) effect refers to the phenomenon where urban temperatures are notably higher compared to surrounding rural areas [1]. Historical UHI data indicate London has experienced rising temperatures since the late 19th century, with hotter summers and a widening temperature gap with its surrounding areas. [2]. After the Industrial Revolution, rapid urban population growth, extensive construction and road paving, industrial activities, and anthropogenic heat discharge have escalated. The accelerating urbanization and rapid industrialization have made UHIs a global environmental concern. In the context of global warming today [3], the impact of UHIs on the thermal environment in residential areas can sometimes be more direct than the effects of climate change [4], and there is a mutual influence between the two [5]. Excessive temperatures in cities can imbalance the body's regulatory functions (especially in the elderly) and increase the incidence of diseases such as heart attacks and pyrexia. For every 1 K rise in temperature, the number of heat-related deaths in people over 65 years of age is expected to double [6]. At the same time, the heat island effect reduces human living comfort, and residents will consequently consume 2–4% more energy for cooling for every 1 °C rise, creating a vicious cycle [7,8].

Since the 20th century, the link strategy of the heat island effect has received more and more attention. The mitigation methods of the heat island effect can reduce the temperature up to 1.5–2.0 K on average, which is important for urban policy making and sustainable development [9,10]. The denser the building complex in a city, the greater the warming effect, and the more open the urban design, the less likely it is to gather heat [11]. In response to the challenge of the UHI effect, greening mitigation initiatives are also gaining attention. In recent years, London has introduced the All London Green Grid, which continuously integrates green space into the urban fabric to reduce urban temperature by linking green spaces [12]. In Singapore, green spaces are integrated into buildings and cityscapes to create a “garden city” and a cooling urban microclimate [13]. Recent studies have shown that the cooling effect of forests mainly works in two ways. The first is through utilizing the characteristics of the trees themselves to achieve cooling. For example, by using the shading effect of leaves to block shortwave radiation from the sun, reducing ground surface temperatures; by absorbing carbon dioxide through photosynthesis, reducing greenhouse gas emissions, and improving the microclimate in cities; and the transpiration of vegetation can also achieve cooling by increasing air humidity, reducing heat flow in the air, and reducing longwave radiation, among other mechanisms [14–16]. Second is by slowing down the heat island effect through the reasonable allocation of green space across the landscape spatial layout. Existing studies have confirmed that the proportion and distribution characteristics of forests and shrubs in urban areas can significantly reduce the intensity of urban heat islands. The green space aggregation index and the largest patch index are strongly negatively correlated with ground surface temperature, and reasonable forest arrangements can have a certain cooling effect on urban heat islands. In contrast, the reduction of forest areas leads to a harder urban surface, which makes the urban ground more prone to absorb and store heat, resulting in an exacerbation of the urban heat island effect [17–20].

Around the world, the majority of research aimed at mitigating the UHI effect is concentrated in densely populated and economically advanced regions [21–24]. Recent studies have infrequently addressed how aspects such as urban layout and green space planning impact UHIs, in which environmental conditions and socioeconomic development levels differ significantly. This paper focuses on Yan'an, a tier-3 city in China known for its significant ecological improvements over the past two decades. This city represents the kind of place that has not seen much research on how to relieve the heat island effect. There is a lack of research concerning the mitigation of UHI effects in similar cities. This research is significant for the development of small and mid-sized cities as it fills the gap in sustainable studies related to strategic land use planning and urban climate management for these regions. Through GIS technology, the study deeply analyzes the state of urban vegetation coverage and the spatial distribution changes of the UHI. It reveals how changes in vegetation affect the temporal and spatial characteristics of the UHI. Qualitative analysis of how vegetation eases the UHI effect in Yan'an fills the gap in research on forests' ability to counter UHIs in less developed areas. Additionally, it compares different types of vegetation to identify the most effective ones for cooling. This research highlights the potential value of various plantings in alleviating the UHI effect, providing theoretical support for greening strategies—like the pattern, area, and distribution of plants in underdeveloped regions. The forests in Yan'an are primarily artificial, dense, and lie at some distance from the city center, raising questions about their temperature regulatory capabilities. This study uses the NDVI and LST data for analysis and modeling. It shows how the forest's cooling effect relates to its distance from the city and identifies an effective range of this cooling. The paper not only explores the value and effectiveness of artificial forests in mitigating the UHI effect but also informs city planning and ecological strategies for less developed regions.

2. Materials and Methods

2.1. Study Area

The study area is Yan'an City (Figure 1), selected for its distinct climatic conditions and ecological significance. Yan'an City, a renowned historical city with a resident population of about 2,282,581 and an urbanization rate of 61.97%, represents an ideal urban case for studying heat island effects due to its typical temperate monsoon climate and rapid urbanization spells, positioned as a third-tier city in China. The geographical coordinates of Yan'an City range between $109^{\circ}13' \sim 110^{\circ}49' E$ and $36^{\circ}25' \sim 37^{\circ}35' N$, with a total area of 37,031.3 square kilometers. Because of its diverse vegetation types and distribution, it is known as the “one of the lungs of Shaanxi”. According to the survey data released by the Forestry Bureau, the total area covered by forests in Yan'an City is about 19,652.5 square kilometers as of 2022, with a coverage rate of 53.07%, and the total volume of standing trees has reached 86,966,000 cubic meters, most of which are the forests on the mountain ranges, and there are also small urban green islands such as Ganquan Laoshan Forest Park, etc. During the period of 2017–2022, a total of 38,555.10 square kilometers of afforestation area was completed in Yan'an City. Yan'an City is within the scope of the Three-North Project, which is known as “the world's largest ecological project”. Since the implementation of various ecological restoration projects, the city has continuously realized the “double increase” in forest accumulation and resource area [25,26] and has been one of the cities with the fastest growth of vegetation cover.

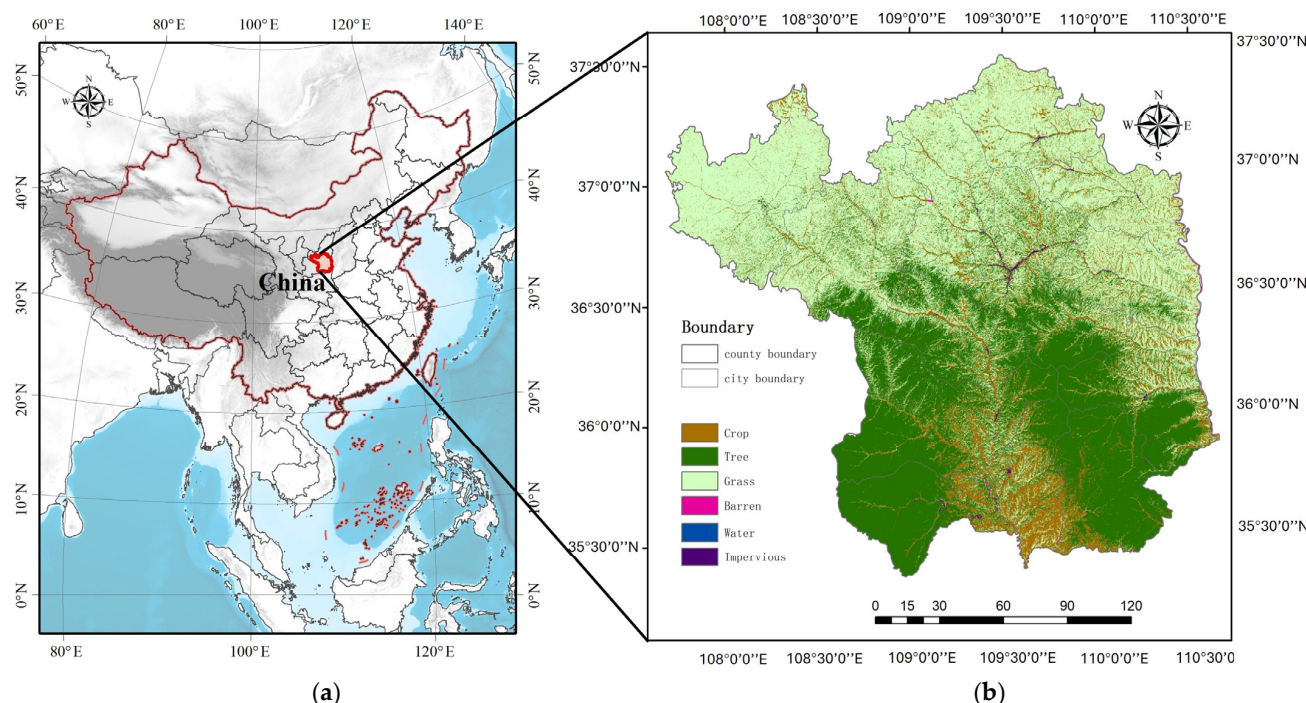


Figure 1. Study Area. (a) Location of the study area in China; (b) Land Use and Land Cover of Yan'an City in 2017.

Yan'an City, located in the northern part of Shaanxi Province and in the middle of the Loess Plateau, represents the typical transitional zone between arid and semi-arid regions, making it particularly sensitive to UHIs. It is connected to Yulin in the north, Xianyang, Tongchuan, and Weinan cities in the south, and bordered by the Yellow River and Shanxi in the east and Gansu in the west. Yan'an has a temperate monsoon climate and belongs to the arid and semi-arid transition zone of China, which makes the city conducive to studying the interaction between vegetation dynamics and UHI mitigation. The main climatic characteristics include abundant light and heat resources, dryness, little rain, strong evaporation, and a large temperature difference between day and night, with

average annual temperature of 9.9 °C and total annual precipitation of 507.7 mm. The study area is characterized by a wide range of round hills and valleys, a high terrain in the north and a low terrain in the south, and major mountain ranges such as the Baiyu Mountains, the Ziwuling Mountains, and the Huanglong Mountains, with a fragmented surface, large undulations and steep slopes, and significant spatial variations in temperature and precipitation, which have an important influence on the distribution of vegetation cover.

2.2. Methodological Framework

This study aims to investigate the mitigating effects of forest on the UHI effect in Yan'an City, delineating the methodological approach into three distinct stages. First, LST and NDVI data from MODIS products were downloaded, as well as county and municipal administrative boundaries and annual land cover datasets with a spatial resolution of 30 m. The analysis phase consisted of examining vegetation changes, changes in heat island areas and their intensity, and correlations between NDVI and LST. This phase also included the creation of buffer zones around the affected areas to study the effect of the distance of forests in mitigating UHIs. Ultimately, the results of the study demonstrated the spatial and temporal effects of vegetation on UHIs, identified the most effective types of vegetation mitigation, and determined the effective range of forests in mitigating UHIs. The results of the study provide a basis for decision making on forest layout and ecological conservation strategies in Yan'an City. Figure 2 illustrates the flowchart of this paper.

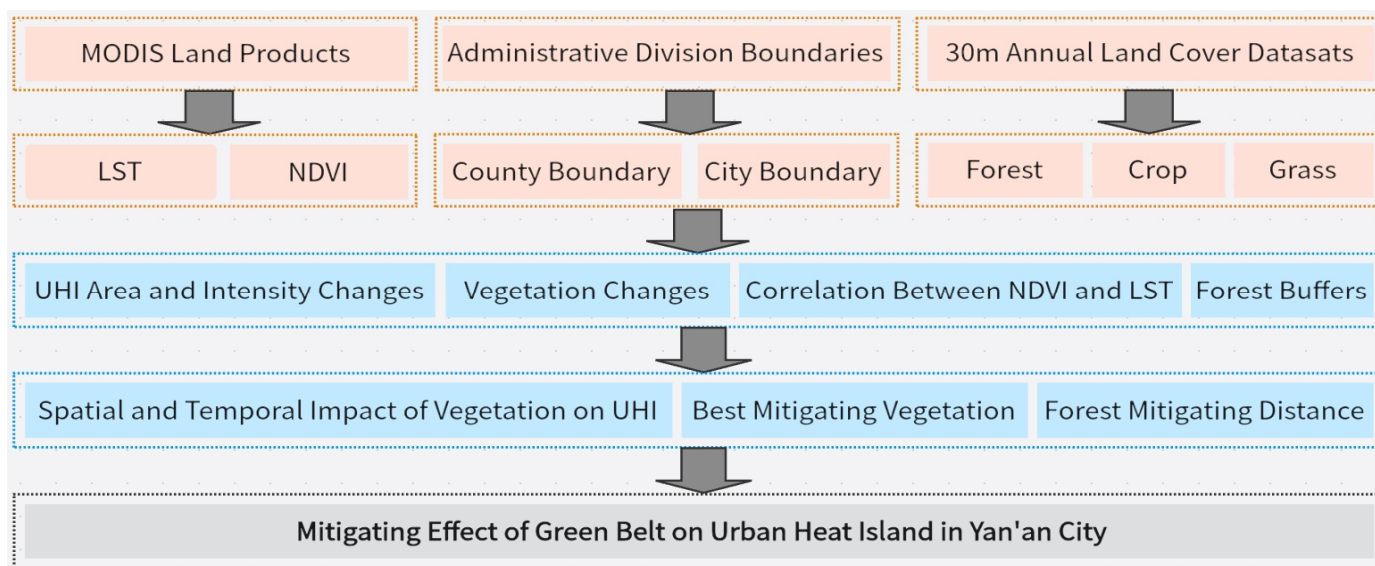


Figure 2. Flowchart of the data used in the article. This figure shows how they were utilized in a step-by-step manner to ultimately arrive at the conclusions.

2.3. Data Sources

2.3.1. MODIS Land Products

MODIS is suitable for mesoscale urban heat island studies. A large volume of UHI-related research uses it because of its free access, easy acquisition, and wide coverage [27–31]. MODIS is equipped with two types of sensors, Terra and Aqua. The Aqua sensor has a temporal resolution of 8 days and a spatial resolution of 1000 m, with overpass times at approximately 1:30 p.m. and 1:30 a.m. Compared to the Terra sensor, the daytime temperatures captured by Aqua are very close to the highest temperatures of the day, making it ideal for extracting heat island regions [31,32]. This study uses the L3 MODIS LST product (MYD11A1) and the L3 MODIS NDVI product (MYD13Q1) from 2017 to 2022. Both are located within the same coordinate system (WGS 84) but they have different spatial resolutions. It is necessary to resample the LST product through spatial interpolation methods to match the spatial

resolution of the NDVI product. Table 1 gives basic information about the MODIS data used in this research.

Table 1. MODIS Land Products and Relevant Properties.

MODIS Land Products	Date	Band	Resolution (M)
MYD11A1	2017-06-01 to 2017-08-31	LST_Day_1km	1000
	2018-06-01 to 2018-08-31		
	2019-06-01 to 2019-08-31		
	2020-06-01 to 2020-08-31		
	2021-06-01 to 2021-08-31		
	2022-06-01 to 2022-08-31		
MYD13Q1	2017-06-02, 2017-06-18, 2017-07-04, 2017-07-20, 2017-08-05, 2017-08-21 2018-06-02, 2018-06-18, 2018-07-04, 2018-07-20, 2018-08-05, 2018-08-21 2019-06-02, 2019-06-18, 2019-07-04, 2019-07-20, 2019-08-05, 2019-08-21 2020-06-01, 2020-06-17, 2020-07-03, 2020-07-19, 2020-08-04, 2020-08-20 2021-06-02, 2021-06-18, 2021-07-04, 2021-07-20, 2021-08-05, 2021-08-21 2022-06-02, 2022-06-18, 2022-07-04, 2022-07-20, 2022-08-05, 2022-08-21	NDVI	250
	2020-06-01, 2020-06-17, 2020-07-03,		
	2020-07-19, 2020-08-04, 2020-08-20		
	2021-06-02, 2021-06-18, 2021-07-04,		
	2021-07-20, 2021-08-05, 2021-08-21		
	2022-06-02, 2022-06-18, 2022-07-04,		
	2022-07-20, 2022-08-05, 2022-08-21		
	2020-06-01, 2020-06-17, 2020-07-03,		
	2020-07-19, 2020-08-04, 2020-08-20		
	2021-06-02, 2021-06-18, 2021-07-04,		
	2021-07-20, 2021-08-05, 2021-08-21		
	2022-06-02, 2022-06-18, 2022-07-04,		
	2022-07-20, 2022-08-05, 2022-08-21		

This article utilized the GEE platform to retrieve the MYD11A1 and MYD13Q1 datasets, selecting the LST and NDVI products from June to August (summer in Yan'an) for annual compounding, mosaicking, clipping, and temperature conversion before downloading. The specific steps are as follows: (1) Load the corresponding date's LST/NDVI dataset in the GEE platform. (2) Import the research area vector file and clip the imagery. (3) For the LST dataset, it is also necessary to convert the temperature values to degrees Celsius. The mean composite method ensures the spatial integrity of the data. The urban heat island effect is strongest and the vegetation growth condition is optimal in summer. This meets the requirements of this article to quantify the interannual variation of the urban heat island and to understand its association with vegetation. Figure 3 shows that June-August is the period of the year with the highest temperatures in the city of Yan'an, and it is summer in Yan'an.

2.3.2. China Land Cover Dataset (CLCD)

The CLCD used in this study [33] is based on a comprehensive assembly of 335,709 Landsat images on the GEE. This has led to the creation of the first Landsat-derived annual CLCD. The training samples were collected by combining stable samples extracted from the CLCD with visual interpretation samples from satellite time-series data, Google Earth, and Google Maps imagery. Several temporal indicators were constructed using all available Landsat satellite data, and these were fed into a random forest classifier to obtain classification results. To enhance the temporal and spatial consistency of the CLCD, a post-processing method incorporating spatiotemporal filtering and logical reasoning was proposed. This dataset was employed to delineate the land use types within Yan'an City by downloading six phases of land use type coverage data for the years 2017 to 2022. The land use types of forests, croplands, and grasslands in Yan'an City were extracted using the ArcGIS 10.8 software for mosaicking and clipping and then resampled to a 250 m resolution to ensure consistency with the spatial resolutions of NDVI and LST data.

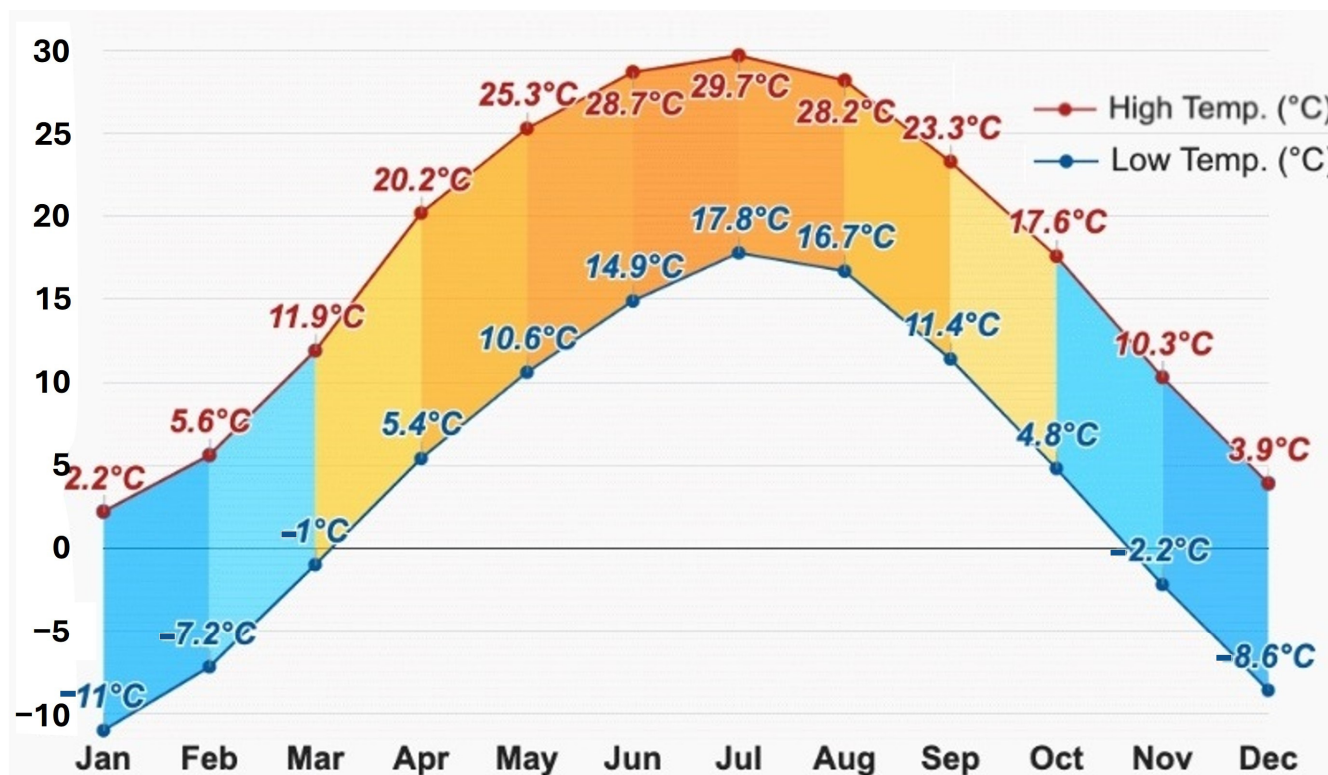


Figure 3. Monthly average maximum and minimum temperatures in Yan'an City.

2.3.3. Statistical Data

This study uses new afforestation area data from 2017 to 2022 from the Shaanxi Provincial Statistical Yearbook issued by the Shaanxi Provincial Bureau of Statistics, obtained through the official website of the organization (<http://tjj.shaanxi.gov.cn/tjsj/ndsj/tjn/>), accessed on 17 March 2024), which contains in its dataset the specific camping area of Yan'an City for the period of 2017–2022 and the camping area under different afforestation methods, which are credible and authoritative.

2.4. Processing Methods

2.4.1. Calculate NDVI

NDVI is widely used to assess the quantitative value of vegetation cover and is one of the most suitable indices for monitoring crop growth dynamics. The NDVI was calculated by the following Equation (1):

$$\text{NDVI} = \frac{(\text{NIR} - \text{RED})}{(\text{NIR} + \text{RED})} \quad (1)$$

According to existing research, the peak values of NDVI occur during the summer each year, representing the maximum level of vegetation cover throughout the year [34]. This study extracts NDVI data from the peak growing season for trend analysis, rather than aggregate NDVI over an entire year. A period from June to August is selected annually from 2017 to 2022, and an average value synthesis is performed for the NDVI of each pixel to determine the maximum NDVI value of Yan'an City within a year. This timeframe minimizes the impact of seasonal changes, as well as climatic and weather disturbances. During the summer, vegetation usually experiences its most vigorous growth; extended daylight hours and suitable temperature conditions create the ideal natural environment for plant growth, leading to the highest biomass and chlorophyll activity and, consequently, the highest annual NDVI values. The larger weather variations in spring and autumn may affect the precision of NDVI, while the relatively stable climate of the summer favors the

acquisition of accurate data, thus more accurately reflecting the health status and coverage of vegetation.

2.4.2. Extraction of UHI Areas and UHI Intensity Calculation

(1) Calculation of LST

The MODIS MYD11A1 dataset provides estimates of LST, which is particularly applicable to the study of the UHI effect. In this case, the ground temperature data in the MODIS product are mathematically linearly transformed before storage and need to be calculated and processed by Equation (2) to obtain the actual value ($^{\circ}\text{C}$):

$$\text{LST} = a \times \text{DN} + b \quad (2)$$

where LST is the land surface temperature, DN is the image pixel value, a is the scaling factor, and b is the offset. In this study, the scaling factor is 0.02 and the offset is -273.15 .

The data thus processed may have negative values, and all negative values need to be processed as Nodata in ArcGIS 10.8 to avoid subsequent result errors.

(2) Extraction of UHI Region

In this study, the mean–standard deviation method was selected to extract the UHI region [35]. The study area of this paper spans five years, and the surface temperatures between different years are not comparable. It is necessary to consider the mean and standard deviation of different years comprehensively and utilize the combination of surface temperature mean and different standard deviation multiples to delineate the surface heat field. The mean value and standard deviation can reflect the variation of temperature in different features, with a more reasonable hierarchical structure and better ability to express details. This can avoid the error caused by the temporal phase difference to a certain extent, and the temperature field in the study area is divided into 4 levels using Table 2 as the standard. The high-temperature area is extracted as the UHI region in Yan'an City.

Table 2. Method for Dividing Land Surface Thermal Field Levels Using Mean–Standard Deviation.

Temperature Field Level	Division Criteria	Colors
High-Temperature Zone	$\text{Ts} > \mu + \text{std}$	
Sub-High-Temperature Zone	$\mu < \text{Ts} \leq \mu + \text{std}$	
Medium-Temperature Zone	$\mu - \text{std} \leq \text{Ts} \leq \mu$	
Low-Temperature Zone	$\text{Ts} < \mu - \text{std}$	

where Ts is the surface temperature; μ is the mean; and std is the standard deviation.

(3) Calculation of surface UHI intensity (SUHII)

The high-temperature area is designated as the UHI region. The UHI intensity for Yan'an City from 2017 to 2022 is calculated as Equation (3):

$$\text{SUHII} = \text{Tu} - \text{Tr} \quad (3)$$

where SUHII represents the UHI intensity, Tu is the annual average LST of the UHI area, and Tr is the annual average temperature of other areas.

2.4.3. Statistical Analysis

(1) Correlation Analysis

The main purpose of correlation analysis is to assess whether there is a linear relationship between two variables and the strength of the relationship. The correlation analysis in this study was conducted in three main steps:

First, “Create Random Points” was used in ArcGIS 10.8. One thousand different random points (six thousand points in total) were extracted from the NDVI and LST images for each year. Second, the ArcGIS 10.8 tool “Extract Multiple Values to Points” was used. Based on the year as the grouping basis, we divided them into six groups and assigned the values calculated by NDVI and LST to the points and exported the results. Thirdly, the data with anomalies or null values were excluded from the results. Based on previous related studies [34], it can be assumed that there is a linear relationship between NDVI and LST. The Pearson correlation coefficient was used to measure the linear relationship between the variables. The value of this coefficient ranges from -1 to 1 , where a positive value indicates positive correlation, a negative value indicates negative correlation, while 0 indicates no linear relationship, and a larger value indicates a more significant correlation, which is calculated as in Equation (4):

$$r = \frac{\sum_{i=1}^n (X_i - \bar{X})(Y_i - \bar{Y})}{\sqrt{\sum_{i=1}^n (X_i - \bar{X})^2} \sqrt{\sum_{i=1}^n (Y_i - \bar{Y})^2}} \quad (4)$$

where, r is the Pearson coefficient, n is the number of samples, i is the year ordering, X_i is the standardized score of NDVI samples and is the sample mean, Y_i is the standardized score of LST samples and is the sample mean. In this study, $n = 6$, 2017 data $i = 1$, plus 1 for each year, and 2022 data $i = 6$.

(2) Overlay Analysis

Overlay analysis is often used to study the relationship between different data layers in geographical space. By combining multiple geographic data layers, the spatial association and influence relationship between various geographical elements can be obtained. In this study, vegetation type and temperature field information were overlaid to analyze changes in the temperature fields of various types of vegetation.

3. Results

3.1. Interannual Variation of NDVI and Vegetation Coverage in Yan'an City

The NDVI is very sensitive to the biophysical characteristics of vegetation. It objectively discloses critical information like vegetation cover and growth conditions on a rather extensive spatiotemporal scale. In this study, we have extracted the NDVI value for Yan'an City from MODIS terrestrial products. NDVI values range from -1 to 1 , with water bodies exhibiting a negative value. Bare land/wasteland and developed areas have lesser values and are collectively referred to as non-vegetation areas ($NDVI \leq 0.2$) [36,37]. Areas with an NDVI value greater than 0.2 are defined as vegetation areas. Substantial positive values usually symbolize healthy green vegetation. In this paper, we have integrated data of land use and cover type, defining areas with $NDVI \geq 0.4$ as zones with healthy vegetation growth. Based on the above rules, reclassification was conducted and the area and ratio of each category were statistically analyzed. The result indicates that the overall vegetation coverage in Yan'an City is exceptionally high, surpassing 95%. Except for 2017, the proportion of regions with good vegetation growth has always exceeded 60%. Table 3 presents the areas of each value domain.

Spatial distribution maps of different numerical levels in Yan'an City from 2017 to 2022 were created by ArcGIS 10.8. As can be seen from Figure 4, the spatial distribution of vegetation in Yan'an City varies prominently between the six years, overall displaying a “higher in the south and lower in the north” pattern. Well-growing areas (represented in olive green and dark green) have been gradually spreading from the south to the

north of Yan'an City, especially with improved vegetation growth around Baota District. Non-vegetation parts of Yan'an City are concentrated in Baota District and the south and east edges of the city. The distribution of built-up areas follows a pattern of “more in the north and less in the south”, which is opposite to the distribution of vegetation (see Figures 1b and 4). This is consistent with the spatial and temporal variation rule of the Loess Plateau, which presents a pattern of being higher in the south than the north and gradually decreasing from the south to the north. It coincides with the shift of the ecological farming retreat's focus from the northeast to the southwest in Yan'an City [38,39].

Table 3. Proportions and Area of different NDVI value domains in Yan'an City (2017–2022).

Year	2017	2018	2019	2020	2021	2022
NDVI < 0.2 Area (km ²)	1406.97	1139.67	1063.11	1108.05	1030.19	1290.05
0.2 ≤ NDVI < 0.3 Area (km ²)	4797.89	4434.93	4224.29	2810.69	3433.87	3653.89
0.3 ≤ NDVI < 0.4 Area (km ²)	8838.54	9110.37	8189.67	5768.63	6430.16	6491.21
0.4 ≤ NDVI < 0.6 Area (km ²)	16,441.83	15,972.63	15,511.55	18,333.07	16,391.66	15,219.67
NDVI > 0.6 Area (km ²)	5546.07	6373.70	8042.68	9310.08	9745.42	10,376.48

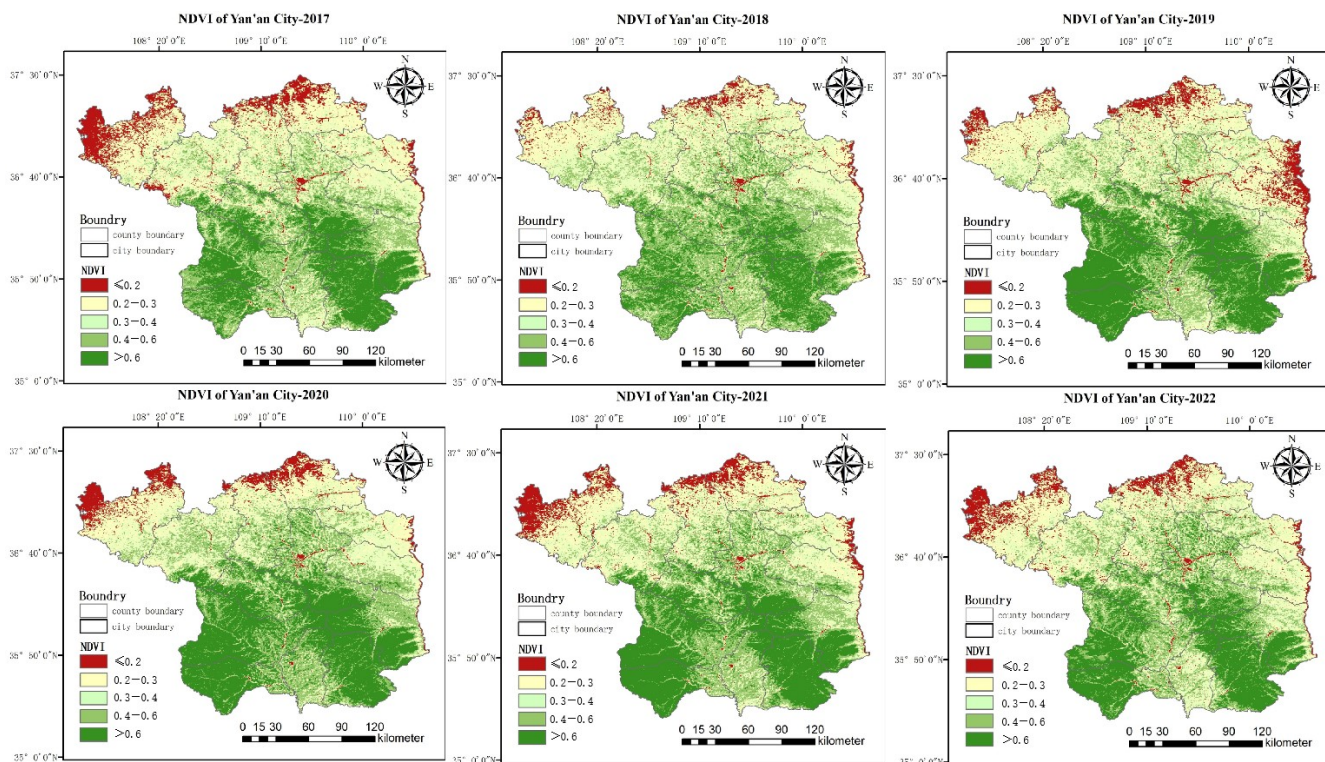


Figure 4. Spatial distribution maps of different numerical levels in Yan'an City from 2017 to 2022.

The northern part of Yan'an City is characterized by loess ridges and gullies, with a dry climate and scarce rainfall, which is not conducive to vegetation growth. In contrast, the southern part consists of low mountains, hills, and plains with a moist climate that is suitable for vegetation growth [40]. As a result, the vegetation cover and quality in Huangling County and Huanglong County in the southern area have always been at a higher level. Meanwhile, due to the impact of ecological restoration projects, the vegetation cover levels and quality within the northern part of Yan'an City, including Zhidan County, Zichang County, and Yanchang County, have been steadily increasing in recent years [41].

In this study, the NDVI values ranged from −0.13 to 0.78 in 2017, −0.11 to 0.82 in 2018, −0.15 to 0.82 in 2019, −0.15 to 0.81 in 2020, −0.12 to 0.83 in 2021, and −0.06 to 0.82 in 2022. Peak values exceeded 0.8 except in 2017, with the average NDVI values increasing from 0.50 to 0.67 and the minimum values increasing from −0.13 to −0.06, as

shown in Figure 5. This indicates overall good vegetation growth during the summer in Yan'an City, with improvements in vegetation coverage, growth conditions, and greenness. After analyzing remote sensing data, it was discovered that peak NDVI values are entirely located within the extensive southern forests along the city's borders as depicted in Figure 4. This demonstrates that vegetation growth conditions are superior in the southern part of Yan'an City compared to the north, aligning with the general distribution pattern of more vegetation cover in the south than the north.

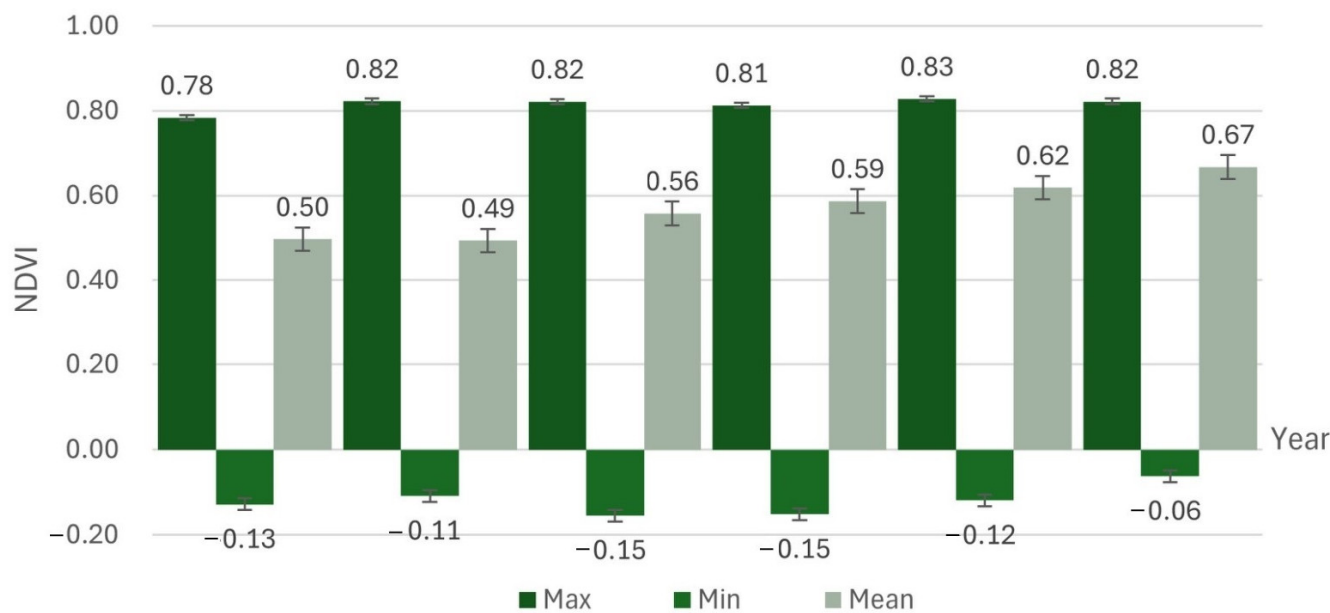


Figure 5. Trend Analysis of Average NDVI in Yan'an City (2017–2022).

Many forests are concentrated within the southern administrative regions of Fuxian County, Huangling County, and Huanglong County, far away from the dense urban construction areas like Baota District and Ansai County. Forest coverage is less within the central urban area, with nearby forest zones being fragmented and distributed among forest parks. According to official statistics, from 2017 to 2022, Yan'an City completed afforestation over an area of 3855.10 km². The afforestation capacity has been consistently high (Table 4) with forest coverage area experiencing a dramatic increase.

Table 4. Annual Incremental Afforestation Area in Yan'an City (2017–2022).

Year	Afforestation Area (km ²)	Forest Type Purpose	
		Economic Forest	Protective Forest
2017	703.53	7.20	554.35
2018	689.72	13.46	384.27
2019	654.76		590.52
2020	221.43	3.37	412.81
2021	775.77		729.71
2022	1003.13		

Combining CLCD and NDVI data, forest, grassland, and cultivated land areas in Yan'an City from 2017 to 2022 were extracted (CLCD represents forest, grassland, and cultivated land, and NDVI ≥ 0.2) [42–44]. The proportion of each type of vegetation is shown in Figure 6. Forests are the land type with the most coverage area in Yan'an City, with a coverage rate that shows an increasing trend year by year, growing from 44.77% to 51.69%, an increase rate of 6.92% over six years. Cultivated land exhibits a slight upward trend, increasing from 8.30% to 8.49%. The proportion of grassland cover increased from 38.14% to 39.94%.

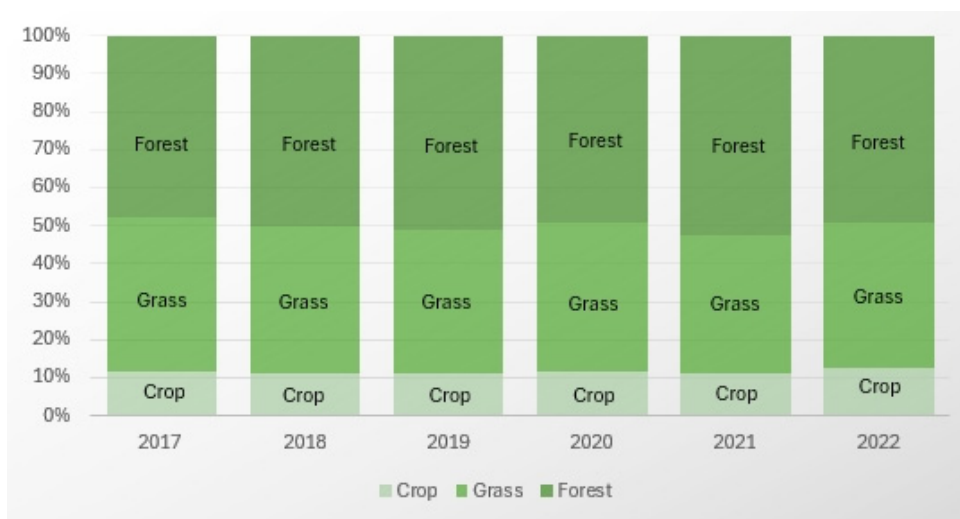


Figure 6. Proportions of each vegetation type in Yan'an City (2017–2022).

The vegetation coverage ratio increased from 84.45% to 93.54%, with a growth rate of 19.08%/6a in Yan'an City. This indicates that Yan'an City had a relatively high level of vegetation coverage originally, and ecological restoration projects were one of the driving factors for the growth of various types of vegetation [45,46].

3.2. Interannual Variation of Temperature Field and UHI in Yan'an City

The temperature field in Yan'an City was divided into four temperature field classes of high-temperature zone, sub-high-temperature zone, medium-temperature zone, and low-temperature zone based on the mean–standard deviation method. Table 5 demonstrates the 2017–2022 classification criteria for the summer temperature field in Yan'an City.

Table 5. Proportions of Vegetated Area and Non-vegetated Area in Yan'an City (2017–2022).

Year	Vegetated Area (km ²)	Proportions (%)	Non-Forested Area (km ²)	Proportions (%)
2017	31,274.56	84.45	5756.74	15.55
2018	29,711.38	80.23	7319.92	19.77
2019	31,115.27	84.02	5916.03	15.98
2020	31,890.30	86.12	5141.00	13.88
2021	33,863.04	91.44	3168.26	8.56
2022	34,638.03	93.54	2393.27	6.46

Between 2017 and 2021, the average surface temperature during the summer in Yan'an City fluctuated and decreased from 32.82 °C to 31.27 °C. The highest average temperature in this six-year span was recorded in 2021 at 32.96 °C, with an average annual change of −1.1%. From the perspective of standard deviation, during the summers from 2017 to 2021, the standard deviation of Yan'an City's surface temperature fluctuated within the range of 2.46–3.45, indicating that the gap between high and low temperatures was relatively stable. As indicated in Table 6, the average surface temperature and standard deviation declined in 2018 and 2022. According to the statistical data, Yan'an City had a greater afforestation effort in 2017 and 2021 (Table 4), suggesting that such changes may be due to anthropogenic factors.

Table 6. Criteria for Division of Temperature Zones in Yan'an City (2017–2022).

Year	Mean	std	High-Temperature Zone	Sub-High-Temperature Zone	Medium-Temperature Zone	Low-Temperature Zone
2017	32.82	3.04	(35.86, +∞)	(32.82, 35.86]	(29.79, 32.82]	(−∞, 29.79)
2018	30.41	2.51	(32.92, +∞)	(30.41, 32.92]	(27.90, 30.41]	(−∞, 27.90)
2019	32.01	3.29	(35.30, +∞)	(32.01, 35.30]	(28.73, 32.01]	(−∞, 28.73)
2020	31.58	3.24	(34.81, +∞)	(31.58, 34.81]	(28.34, 31.58]	(−∞, 28.34)
2021	32.96	3.45	(36.41, +∞)	(32.96, 36.41]	(29.50, 32.96]	(−∞, 29.50)
2022	31.27	2.46	(33.73, +∞)	(31.27, 33.73]	(28.81, 31.27]	(−∞, 28.81)

Table 7 shows the area and proportion of various thermal field grades in Yan'an City from 2017 to 2022. It can be seen that high-temperature zone areas and medium-temperature zone areas show a fluctuating upward trend. The high-temperature zone areas increased by 1.35% over six years, and the medium-temperature zone areas by 6.59% over six years. At the same time, the proportion of sub-high-temperature areas zone decreased, and the proportion of low-temperature zone areas slightly decreased by 0.94% over six years, with the largest decline of 2.68% occurring in 2018. According to the mean–standard deviation method, high-temperature zone areas were extracted as UHI regions. The UHI area saw a significant increase over six years, peaking at 6603.64 square kilometers in 2018. The average temperature of the UHI overall decreased by 2.04 °C, a larger drop than in other areas (1.48 °C). The UHII showed its highest levels from 2019–2021, exceeding 6 °C, but it significantly decreased by 2022.

Table 7. Information on temperature fields and UHI in Yan'an in different years (2017–2022).

Year	2017	2018	2019	2020	2021	2022
High-temperature zone area (km^2)	5742.94	6603.64	5534.25	5917.76	5534.25	6243.97
Proportions (%)	15.51	17.83	14.94	15.98	14.94	16.86
Sub-high-temperature zone area (km^2)	15,071.38	10,894.97	13,677.28	12,698.32	13,677.28	12,916.84
Proportions (%)	40.70	29.42	36.93	34.29	36.93	34.88
Medium-temperature zone area (km^2)	9195.81	13,505.35	11,379.24	11,839.37	11,379.24	11,199.22
Proportions (%)	24.83	36.47	30.73	31.97	30.73	30.24
Low-temperature zone area (km^2)	7021.17	6027.34	6440.54	6575.86	6440.54	6671.27
Proportions (%)	18.96	16.28	17.39	17.76	17.39	18.02
Average temperature in the UHI area ($T_u/^\circ\text{C}$)	37.10	34.35	37.31	36.6251	38.09	35.06
Average temperature in other regions ($T_r/^\circ\text{C}$)	32.07	29.75	31.06	30.5261	31.97	30.59
UHI intensity ($SUHII/^\circ\text{C}$)	5.03	4.60	6.26	6.10	6.12	4.48

Using ArcGIS 10.8 software, the LST images over the six years were reclassified for mapping (see Figure 7). From the maps, the spatial changes in the UHI regions of Yan'an City can be observed. Between 2017 and 2022, the UHI regions in Yan'an City were concentrated in the northern and eastern border areas, as well as in a very small part of Baota District and the south. According to the reclassification results, there was a certain degree of reduction in the UHI areas of Yan'an City. The medium-temperature and low-temperature zone areas are mainly distributed in the southwest and cover a large area, which might be related to the aforementioned conclusion (the vegetation-covered areas in Yan'an City continuously spread northward, and there are large areas of dense forests in the southwestern region).

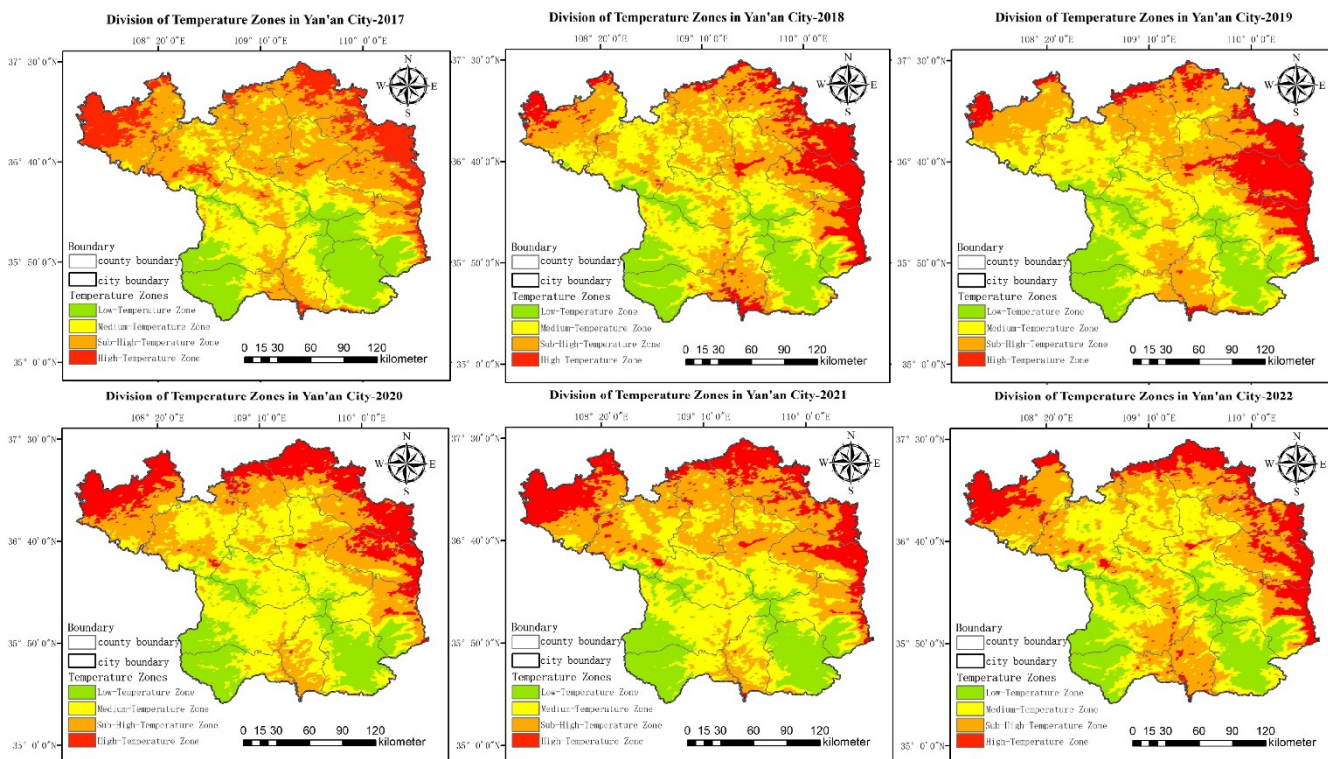


Figure 7. Spatial distribution of different temperature fields in summer in Yan'an (2017–2022).

Further spatial overlay analysis of the LST in Yan'an City from 2017 to 2022 in the summer was conducted to obtain the characteristics and intensity of changes in LST area during the period. As shown in Figure 8, the areas in Yan'an City where the temperature field grade increased cover a vast area. For example, 73.32% of the city shows a trend of transitioning from a lower temperature zone to a higher one, including the forest-dense areas in the southwest, where temperatures are gradually shifting from the low-temperature zone to the medium-temperature and sub-high-temperature zones. Among the six types of transitions from lower to higher temperature zones in the city, the shift from medium-temperature zone to sub-high-temperature zone has the highest proportion, reaching 25.08%, followed by the transition from sub-high-temperature zone to high-temperature zone, at 20.69%. The areas transitioning from higher-temperature zones to lower ones account for only 0.31%, noticeably less than the areas transitioning from lower to higher zones. Areas with no change make up 26.37%, mainly consisting of low-temperature and medium-temperature zones, accounting for 6.87% and 6.29%, respectively. The statistical results indicate that in Yan'an City, the high-temperature zone has the smallest area transitioning to other temperature zones, the medium-temperature zone has the largest area transitioning to other zones, with the smallest area transitioning to lower-temperature zones and the largest area changing to the sub-high-temperature zone.

3.3. Impact of Forests on the UIH in Yan'an City

Based on Figures 4 and 7, the spatial distribution patterns of densely vegetated zones and high-temperature zones exhibit a certain degree of correlation, while there is a certain overlap with the lower-temperature zones. Analyzing the spatial changes in the vegetation corresponding to the temperature field in Yan'an City from 2017 to 2022 (Figure 9), it is observed that the area maintaining a low-temperature forest zone remains unchanged at the highest proportion, accounting for 9.63% of all types of changes. Following this is the transition from a medium-temperature grassland zone to high-temperature grassland zone, accounting for 8.68%. The proportion of temperature fields transitioning from low to high is the lowest in forests, while for grasslands, the transition proportions from low to high and high to low are both high. In cultivated lands, transitions from low to high in temperature fields are the most frequent. These results indicate that grasslands and cultivated lands are more susceptible to changes in temperature field levels due to other factors, while forests exhibit a certain stability and are less susceptible to changes in temperature field levels due to other factors.

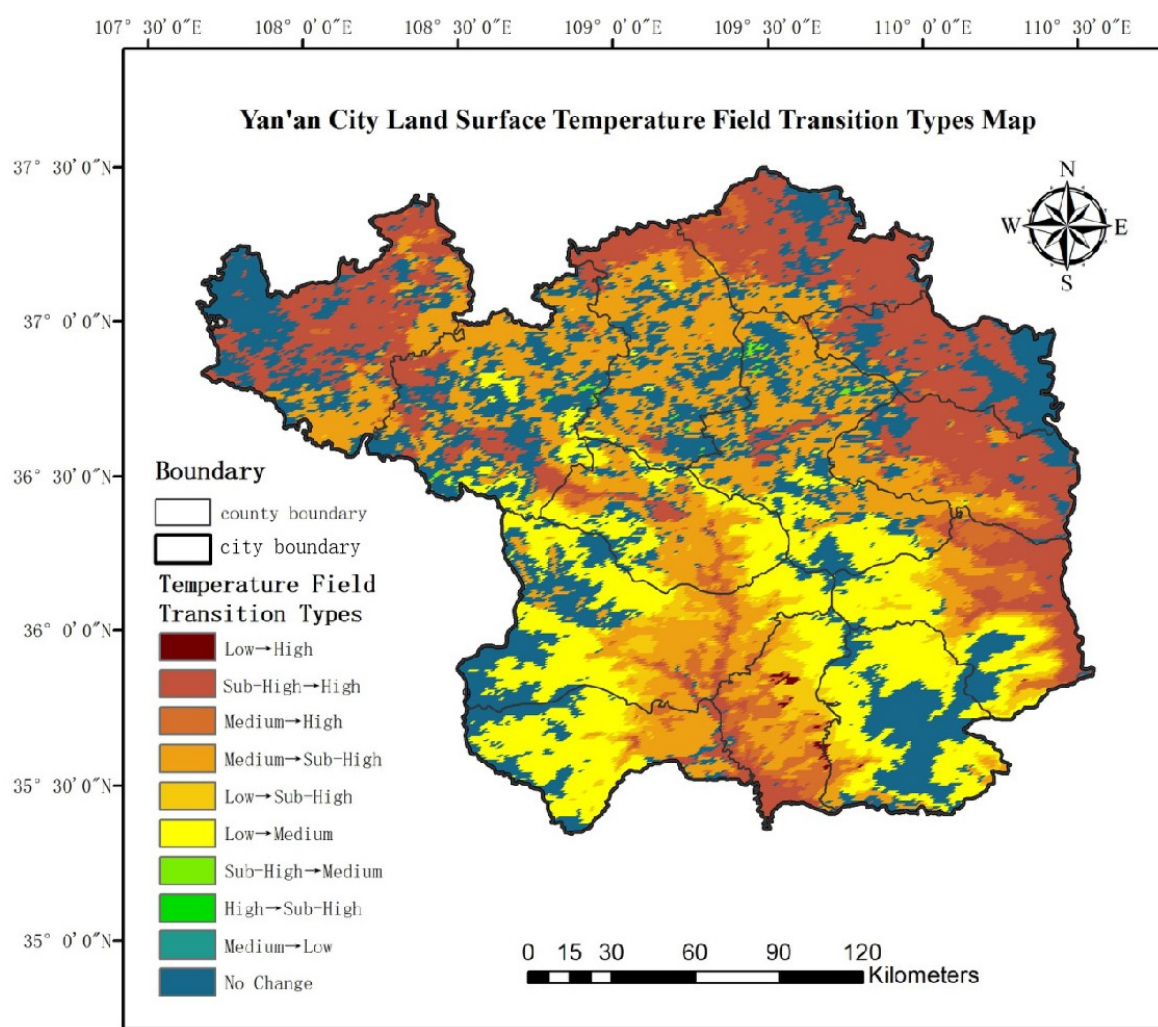


Figure 8. Yan'an City Land Surface Temperature Field Transition Types Map.

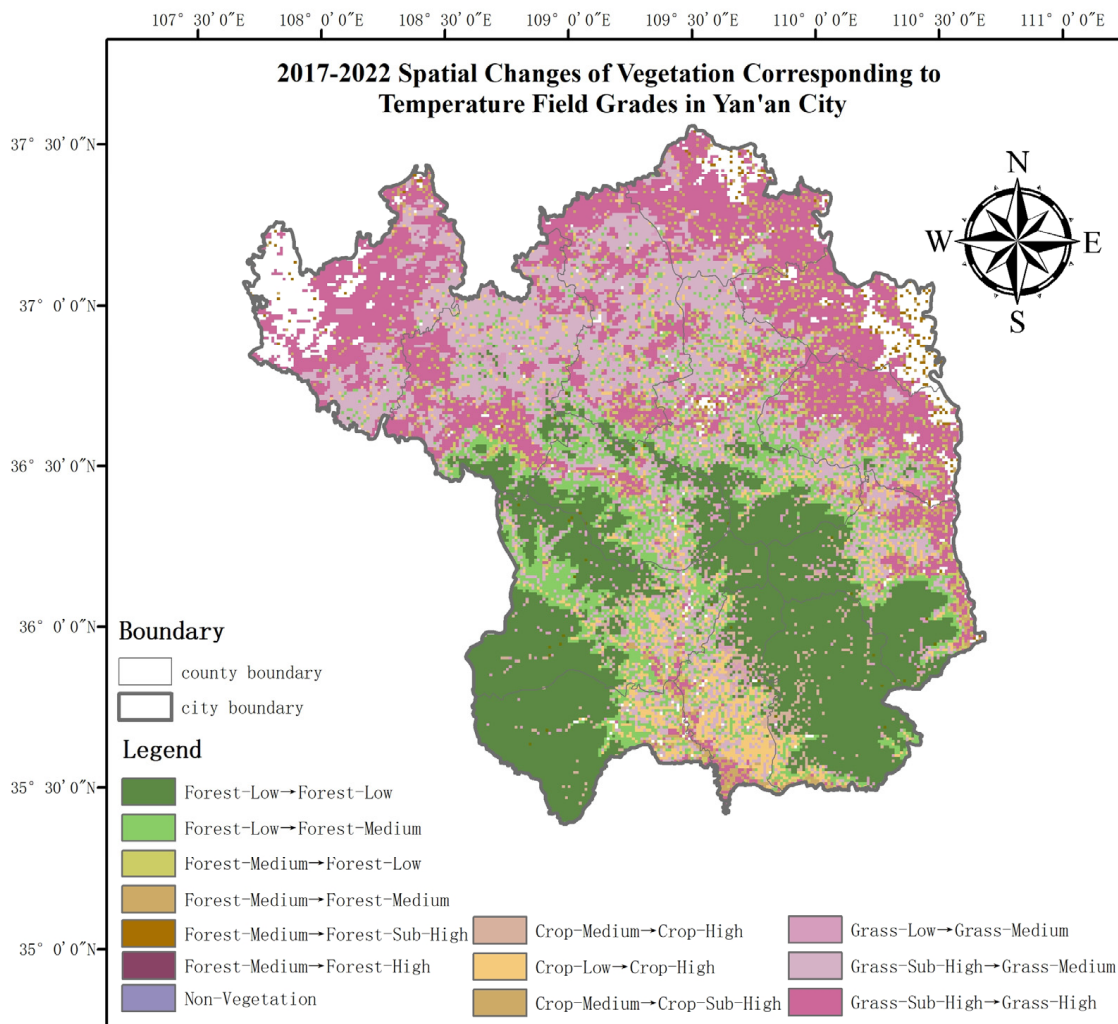
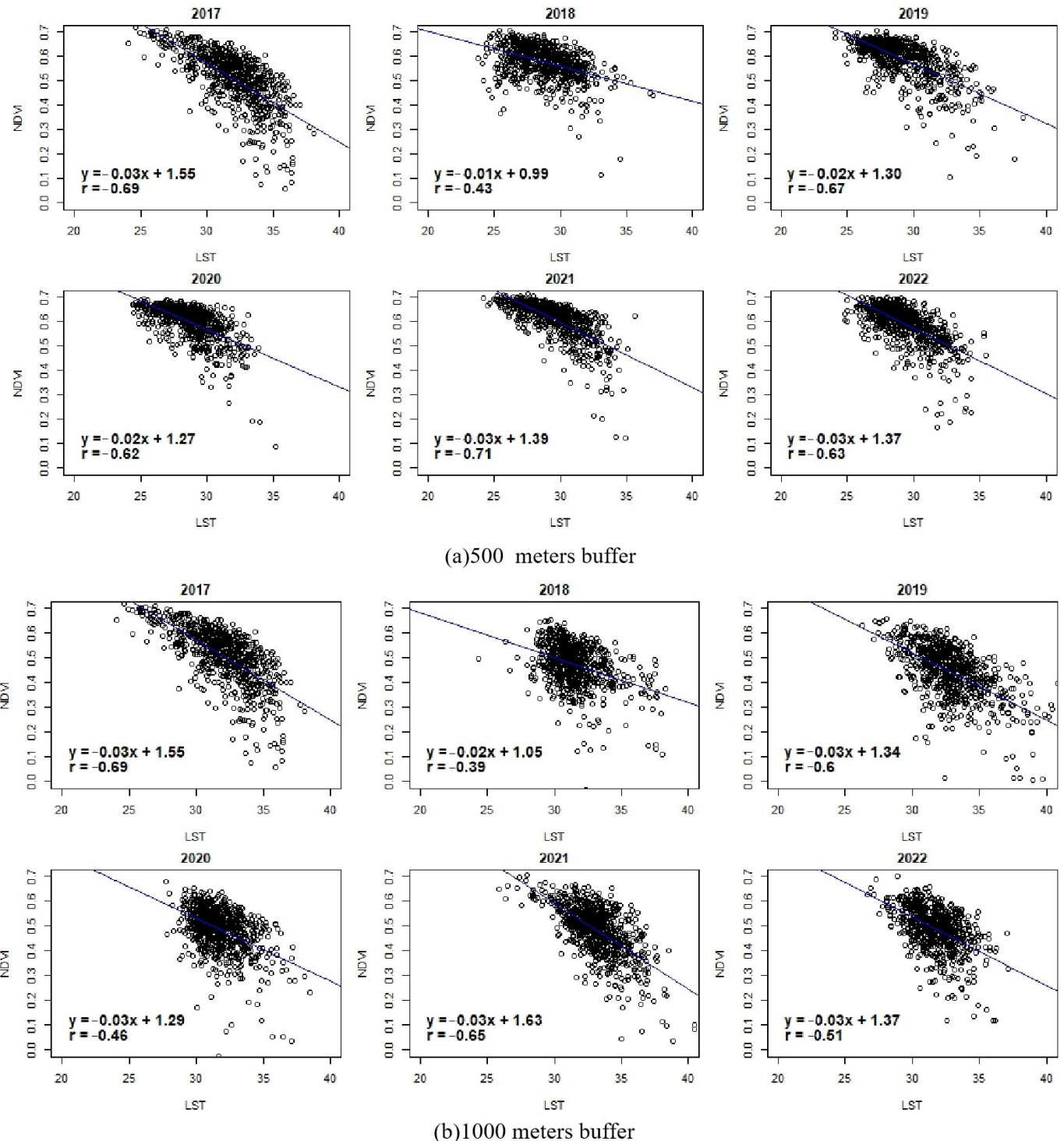


Figure 9. The 2017–2022 Spatial Changes in Vegetation Corresponding to Temperature Field Grades in Yan'an City.

Forests are the most stable vegetation type in Yan'an City, and the cooling effect of forests is analyzed separately. Buffer zones of 500 m, 1000 m, and 2000 m are established around the forest. The correlation analysis of LST and NDVI is conducted within different ranges. Analysis results (Figure 10) show that the slopes of the regression equations within the three buffer zone ranges are all negative, consistent with the calculation results of the correlation coefficient (r), indicating a certain negative correlation between LST and NDVI, i.e., as LST increases, NDVI tends to decrease. For every 1-unit increase in LST, the corresponding NDVI decreases by an average of about 0.02 units. The data analysis within the 500 m buffer zone (Figure 10a) shows that in 2017, 2019, and 2021, the negative correlation between LST and NDVI is more significant, with correlation coefficients of -0.69 , -0.67 , and -0.71 , respectively, and relatively weaker in 2018 ($r = -0.43$). The data analysis within the 1000 m buffer zone (Figure 10b) shows that in 2017, 2019, and 2021, the negative correlation between LST and NDVI is more significant, with correlation coefficients of -0.69 , -0.6 , and -0.65 , respectively, and relatively weaker in 2018 ($r = -0.39$). The data analysis within the 2000 m buffer zone (Figure 10c) shows that in 2017, 2020, and 2021, the negative correlation between LST and NDVI is more significant, with correlation coefficients of -0.41 , -0.35 , and -0.35 , respectively, and relatively weaker in 2018 ($r = -0.17$). Overall, the negative correlation between NDVI and LST in Yan'an City is significant, indicating that forests have a noticeable inhibitory effect on temperature rise and can mitigate the urban heat island effect to a certain extent.

**Figure 10.** Cont.

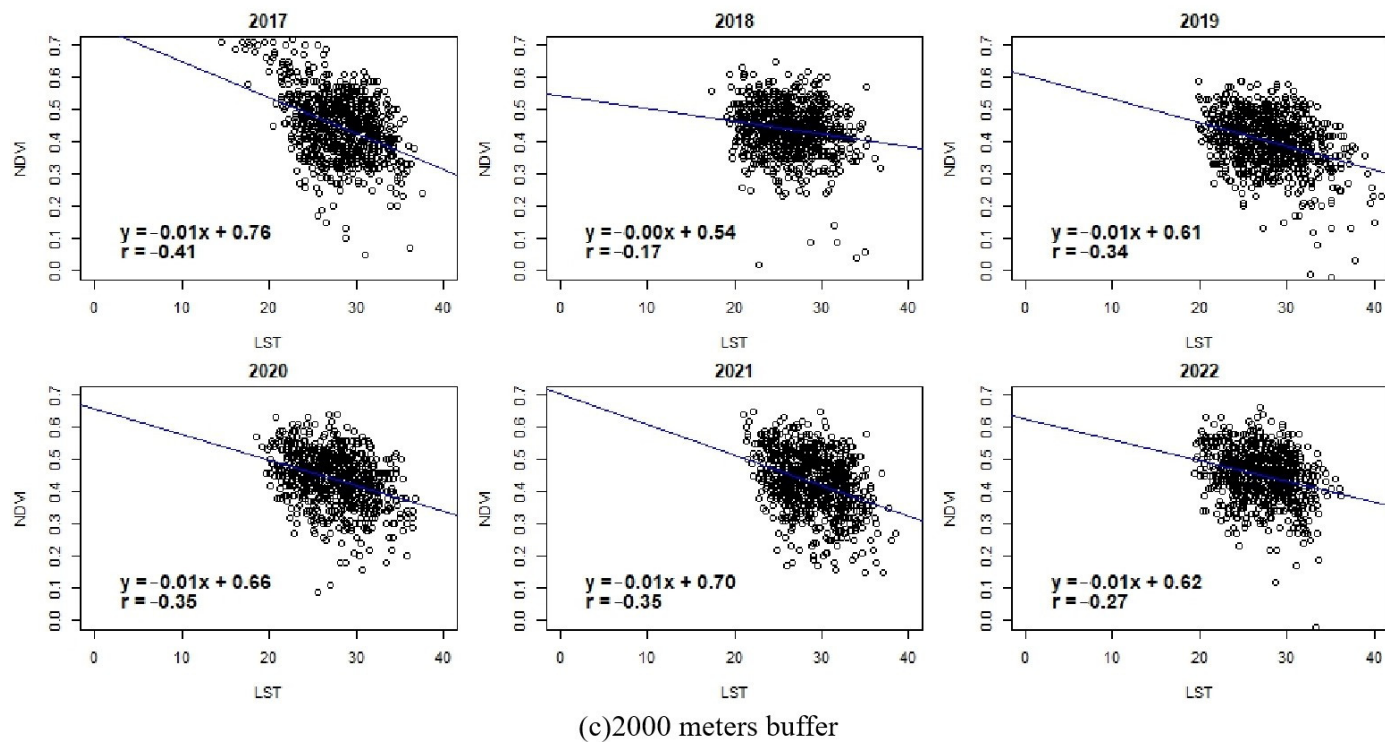


Figure 10. Correlation Analysis of LST and NDVI in Yan'an City (2017–2022).

4. Discussion

Since the ecological restoration project was carried out in Yan'an City in 1999, the ecological environment has changed dramatically. The studies that selected this area as the study area mostly focused on exploring its land use type changes and soil erosion improvement [47–49], and a few studied the impact of its new forest on UHIs, which is one of the innovations of this paper. As the development of megacities is gradually becoming saturated, more attention should be turned to cities with more development potential, and more reasonable urban planning should be carried out for underdeveloped cities with reference to past experiences. According to the conclusion from the results of this paper, the maximum UHI intensity of Yan'an City reaches 6.03°C from 2017–2022, and it is necessary to prevent further intensification of the UHI. The study of vegetation dynamics and the spatial distribution of heat islands in Yan'an has revealed a high rate of vegetation cover within the city and intensification of the UHI over the past six years. Correlation analysis between NDVI and LST demonstrates that increasing greenery contributes positively to the mitigation of the UHI, and forests are particularly effective. Correlation results within various buffer zones indicate that afforestation in the urban periphery is effective in reducing temperature fluctuations, and the mitigation of vegetation is more pronounced when it is closer to green areas. Scientific greening strategies and methods are used to enhance the ecological quality and living environment of cities. In the field of urban planning, this study suggests that planners should plant more trees in areas seriously affected by the heat island effect and consider the design of green spaces based on the relationship between vegetation and the cooling effect distance, employing scientific greening strategies and methods to enhance the ecological quality and living environment of cities. Moreover, from a global perspective, the case of Yan'an contributes to a broader understanding of the role of green spaces in ecological restoration and their ability to improve environmental quality. This provides new perspectives and solutions for the heat island phenomenon and environmental challenges faced by cities at different development levels around the world. This paper focuses on the mitigation of the UHI effect in Yan'an City by the studied forest, which has been applied in Shanghai and Zhengzhou, China and Medan, Indonesia [50–52].

There are some other measures to mitigate the UHI effect, which are summarized in the following three categories:

1. Green roofs, green facades, etc.

These generally feature sun-tolerant plants [53]. Covering some or all of the top floors of buildings with green plants reduces the warming caused by the reflection of sunlight on the buildings. Plant transpiration and soil evaporation cool down the building surface and improve the thermal and urban microclimate of the building, thus mitigating the UHI effect [54].

2. Altering the surface materials of the building

The principle is to reflect or absorb a portion of the thermal radiation. Cooling materials reduce thermal energy and regulate heat gain during convection, conduction, and radiation heat transfer [55]. The cooling power is determined by the radiation emitted and absorbed by the material [56]. Common materials include nanomaterials, photonic materials, plasma, phase change materials, etc.

3. Rationalize the urban pattern

This is performed in order to better evacuate the heat gathered in the city [57–59].

In this paper, we focus on the mitigating effect of vegetation on UHIs, mainly because of the vast area of forest in Yan'an City. Factors such as the construction location, area, and density of forest affect the mitigation effect on the UHI [60,61]. Some studies have shown that increasing the green area near residential areas can increase living comfort [62], and lower temperatures can be capitalized on in terms of house prices [24]. Based on the findings of this paper, it is innovative to consider the cooling distance of forest and the spatial heterogeneity of UHIs as some of the considerations for urban planning. The limited nature of land resources determines that green space cannot be increased indefinitely, while strengthening the rationalization of the spatial layout of forest is necessary. This helps to reduce the differences in the thermal environment of the city and can make the layout of urban green space more balanced, scientific, and sustainable.

This study has conducted a profound analysis of the mitigating effects of forests, yet it still has some limitations. Firstly, although this paper discusses the cooling potential of artificial forests on UHIs, it does not include other variables that might impact UHIs, such as environmental humidity, altitude, and economic factors. Future research should carry out a more diversified analysis to consider these variables. Secondly, due to constraints in data acquisition, the MODIS temperature product data have a large spatial resolution, which could deviate from the actual surface temperatures. Future studies may utilize more precise charged sources of temperature data to enhance the accuracy of temperature assessments. Moreover, the evaluation of the limiting distance for forest cooling effects is not exhaustive, as the analysis only considered three distance points. Future studies could refine the step size to yield more precise results. Lastly, further analysis could be conducted on canopy cover and vegetation health in future research.

5. Conclusions

In exploring the spatiotemporal variability of green spaces in Yan'an City, this study used NDVI calculations to effectively reveal changes in vegetation cover and growth conditions. Vegetation zones ($NDVI \geq 0.2$) and well-growing zones ($NDVI \geq 0.4$) identified in this study exhibit differentiated spatial distribution patterns and reflect the regional characteristic of “more in the south and less in the north”, which aligns with the geographical pattern of Yan'an where the south is suitable for vegetation growth and the north is relatively arid. Overall, the vegetation coverage in Yan'an City is very high, exceeding 95%, and the proportion of well-growing vegetation areas is over 60% in all years except 2017. There is a trend of expansion towards the north in both the vegetation-covered areas and well-growing zones annually, with especially noticeable improvements in the vegetation growth in Baota District. Moreover, the coverage of all types of vegetation in Yan'an City has increased, with the most significant growth observed in forested areas. The overall

vegetation coverage ratio has risen to 19.08% per year, and ecological restoration projects are one of the main drivers of this growth across various vegetation types.

Temperature field analysis indicates that the high-temperature zones of Yan'an City are mainly concentrated on the northern and eastern edges of the city, including Baota District, with some appearances in the southern areas. The area of UHI zones has expanded over six years, peaking at 6603.64 square kilometers in 2018, with an average growth rate of 1.35% per year. The UHII was highest from 2019 to 2021, exceeding 6 °C with a peak at 6.26 °C, followed by a decrease in 2022. The analysis of temperature field transitions shows that the majority of areas (73.32%) transitioned from cold to hot zones, with very few areas (0.31%) transitioning to even hotter zones, indicating a general trend of rising temperatures during this period. Additionally, the coverage of different temperature zones has also changed, with an increase in medium-temperature zones and a slight decrease in sub-high-temperature and low-temperature zones. The largest transition area from medium-temperature zones to other fields suggests that the medium-temperature zone is the primary source of change to other zones, representing the most unstable area that is easily affected by other factors and should therefore be given extra attention in urban planning.

By analyzing and comparing the spatial distribution of vegetation and UHIs in Yan'an City, a certain correlation in their spatial patterns is evident. Among different types of landscapes, such as forests, cultivated lands, and grasslands, forests exhibit the most stability against temperature field type changes and effectively mitigate the UHI effect. Further correlative analysis reveals a significant negative correlation between NDVI and LST, signifying that vegetation considerably suppresses a rise in temperature. The relationship between LST and NDVI also varies with spatial scale, where the negative correlation is more significant within 500 and 1000 m of forested regions and weaker within a 2000 m range, demonstrating that the cooling effect of forests is more pronounced when closer to them, with an effective range extending beyond 1000 m. This finding has implications for future urban planning—it is recommended to adjust the urban green space planning to enhance forest, which can help mitigate the urban heat island phenomenon.

Author Contributions: Concepts, Methods, Software, Validation, Formal analysis, Investigation, Writing—original draft preparation, Writing—review and editing, X.W.; Visualization, X.W., Y.C. and B.X.; supervision, Z.W.; funding acquisition, Z.F. All authors have read and agreed to the published version of the manuscript.

Funding: This research was funded by Foundation 55 at Beijing Forestry University (340/GK112301013) and the Natural Science Foundation of Beijing (8232038, 8234065) and the Key Research and Development Projects of Ningxia Hui Autonomous Region (2023BEG02050) and Chongli District Forest Intelligent Fire Protection–Forest Fire Danger Weather Level Prediction and Forecast in Chongli District (No: 2020SLZHFH-1).

Institutional Review Board Statement: Not applicable.

Informed Consent Statement: Not applicable.

Data Availability Statement: The data presented in this study are available on request from the corresponding author.

Acknowledgments: Special thanks to the reviewers for their helpful comments and suggestions.

Conflicts of Interest: The authors declare no conflicts of interest.

Abbreviations

CLCD	China Land Cover Dataset
NDVI	normalized difference vegetation index
LST	land surface temperature

UHI	urban heat island
UHII	urban heat island intensity
MODIS	moderate resolution imaging spectroradiometer
GEE	Google Earth Engine

References

1. Oke, T.R. The energetic basis of the urban heat island. *Q. J. R. Meteorol. Soc.* **1982**, *108*, 1–24. [[CrossRef](#)]
2. Benjamin, K.; Luo, Z.; Wang, X. Crowdsourcing Urban Air Temperature Data for Estimating Urban Heat Island and Building Heating/Cooling Load in London. *Energies* **2021**, *14*, 5208. [[CrossRef](#)]
3. Yoro, K.O.; Daramola, M.O. CO₂ emission sources, greenhouse gases, and the global warming effect. *Adv. Carbon Capture* **2020**, *3*, 28.
4. Tam, B.Y.; Gough, W.A.; Mohsin, T. The impact of urbanization and the urban heat island effect on day to day temperature variation. *Urban Clim.* **2015**, *12*, 1–10. [[CrossRef](#)]
5. Cheng, Z.; Yang, X.; Sun, C.; Xu, Y. Summer Urban Heat Island Variation in Chengdu and Its Relationship with Urban Developmen (in Chinese). *Clim. Chang. Res.* **2016**, *12*, 322–331.
6. Tan, J.; Zheng, Y.; Song, G.; Kalkstein, L.S.; Kalkstein, A.J.; Tang, X. Heat wave impacts on mortality in Shanghai, 1998 and 2003. *Int. J. Biometeorol.* **2007**, *51*, 193–200. [[CrossRef](#)] [[PubMed](#)]
7. Buchin, O.; Hoelscher, M.-T.; Meier, F.; Nehls, T.; Ziegler, F. Evaluation of the health-risk reduction potential of countermeasures to urban heat islands. *Energy Build.* **2016**, *114*, 27–37. [[CrossRef](#)]
8. Tsoka, S.; Tsikaloudaki, K.; Theodosiou, T.; Bikas, D. Urban Warming and Cities’ Microclimates: Investigation Methods and Mitigation Strategies—A Review. *Energies* **2020**, *13*, 1414. [[CrossRef](#)]
9. Manoli, G.; Fatichi, S.; Schläpfer, M.; Yu, K.; Crowther, T.W.; Meili, N.; Burlando, P.; Katul, G.G.; Bou-Zeid, E. Magnitude of urban heat islands largely explained by climate and population. *Nature* **2019**, *573*, 55–60. [[CrossRef](#)]
10. Al-Saadi, L.M.; Jaber, S.H.; Al-Jiboori, M.H. Variation of urban vegetation cover and its impact on minimum and maximum heat islands. *Urban Clim.* **2020**, *34*, 100707–100717. [[CrossRef](#)]
11. Oke, T.R. Street Design and Urban Canopy Layer Climate. *Energy Build.* **1988**, *11*, 103–113. [[CrossRef](#)]
12. Oh, Y. All London Green Grid as Nature-Based Solutions for Urban Resilience. In *The Palgrave Handbook of Climate Resilient Societies*; Springer International Publishing: Cham, Switzerland, 2020; pp. 1–23.
13. Wong, N.H.; Tan, C.L.; Kolokotsa, D.D.; Takebayashi, H. Greenery as a mitigation and adaptation strategy to urban heat. *Nat. Rev. Earth Environ.* **2021**, *2*, 166–181. [[CrossRef](#)]
14. Akbari, H.; Pomerantz, M.; Taha, H. Cool surfaces and shade trees to reduce energy use and improve air quality in urban areas. *Sol. Energy* **2001**, *70*, 295–310. [[CrossRef](#)]
15. Malys, L.; Musy, M.; Inard, C. Direct and Indirect Impacts of Vegetation on Building Comfort: A Comparative Study of Lawns, Green Walls and Green Roofs. *Energies* **2016**, *9*, 32–52. [[CrossRef](#)]
16. Lai, D.; Liu, W.; Gan, T.; Liu, K.; Chen, Q. A review of mitigating strategies to improve the thermal environment and thermal comfort in urban outdoor spaces. *Sci. Total Environ.* **2019**, *661*, 337–353. [[CrossRef](#)] [[PubMed](#)]
17. Yujie, R.; Tang, X.; Fan, T.; Kang, D. Does the spatial pattern of urban blue–green space at city-level affects its cooling efficiency? Evidence from Yangtze River Economic Belt, China. *Landsc. Ecol. Eng.* **2023**, *19*, 363–379. [[CrossRef](#)]
18. Amani-Beni, M.; Zhang, B.; Xie, G.-D.; Shi, Y. Impacts of Urban Green Landscape Patterns on Land Surface Temperature: Evidence from the Adjacent Area of Olympic Forest Park of Beijing, China. *Sustainability* **2019**, *11*, 513–529. [[CrossRef](#)]
19. Cheng, X.; Wei, B.; Chen, G.; Li, J.; Song, C. Influence of Park Size and Its Surrounding Urban Landscape Patterns on the Park Cooling Effect. *J. Urban Plan. Dev.* **2015**, *141*, A4014002. [[CrossRef](#)]
20. Chen, H.; Gu, L.; Lai, Y.Q.; Mu, C.L. Relationship between urban forest pattern and UHI effect in Chengdu city (in Chinese). *Acta Ecol. Sin.* **2009**, *28*, 4865–4874.
21. Li, P.; Siddique, M.A.; Fan, B.; Huang, H.; Liu, D. Impact of Changes in Underlying Surface Cover Types on Urban Heat Islands: A Case Study of Chaoyang District, Beijing. *J. Beijing For. Univ.* **2020**, *42*, 99–109. (In Chinese)
22. Peng, B.; Shi, Y.; Wang, H.; Wang, Y. The impacting mechanism and laws of function of urban heat islands effect: A case study of Shanghai. *Acta Geogr. Sin.* **2013**, *68*, 1461–1471. (In Chinese)
23. Maharjan, M.; Aryal, A.; Man Shakya, B.; Talchhabadel, R.; Thapa, B.R.; Kumar, S. Evaluation of Urban Heat Island (UHI) Using Satellite Images in Densely Populated Cities of South Asia. *Earth* **2021**, *2*, 86–110. [[CrossRef](#)]
24. Hsu, A.; Sheriff, G.; Chakraborty, T.; Manya, D. Disproportionate exposure to urban heat island intensity across major US cities. *Nat. Commun.* **2021**, *12*, 2721. [[CrossRef](#)] [[PubMed](#)]
25. Zhang, K.; Lv, Y.; Fu, B. Vegetation restoration in typical areas of the Loess Plateau and its impact on ecosystem services (in Chinese). *J. Ecol. Rural. Environ.* **2017**, *33*, 23–31.
26. Sun, Y.J.; Ren, Z.Y.; Hao, M.Y.; Duan, Y.F. Spatial and temporal changes in the synergy and trade-off between ecosystem services, and its influencing factors in Yanan, Loess Plateau (in Chinese). *Acta Ecol. Sin.* **2019**, *39*, 3443–3454.
27. Das, P.; Vamsi, K.S.; Zhenke, Z. Decadal variation of the land surface temperatures (LST) and urban heat island (UHI) over Kolkata City projected using MODIS and ERA-interim DataSets. *Aerosol Sci. Eng.* **2020**, *4*, 200–209. [[CrossRef](#)]

28. Monteiro, F.F.; Gonçalves, W.A.; Andrade, L.d.M.B.; Villavicencio, L.M.M.; dos Santos Silva, C.M. Assessment of Urban Heat Islands in Brazil based on MODIS remote sensing data. *Urban Clim.* **2021**, *35*, 100726. [[CrossRef](#)]
29. Si, M.; Li, Z.-L.; Nerry, F.; Tang, B.-H.; Leng, P.; Wu, H.; Zhang, X.; Shang, G. Spatiotemporal pattern and long-term trend of global surface urban heat islands characterized by dynamic urban-extent method and MODIS data. *ISPRS J. Photogramm. Remote Sens.* **2022**, *183*, 321–335. [[CrossRef](#)]
30. Pede, T.; Mountrakis, G. An empirical comparison of interpolation methods for MODIS 8-day land surface temperature composites across the conterminous United States. *ISPRS J. Photogramm. Remote Sens.* **2018**, *142*, 137–150. [[CrossRef](#)]
31. Liu, J.; Hagan, D.F.T.; Liu, Y. Global Land Surface Temperature Change (2003–2017) and Its Relationship with Climate Drivers: AIRS, MODIS, and ERA5-Land Based Analysis. *Remote Sens.* **2020**, *13*, 44–64. [[CrossRef](#)]
32. Qiao, Z.; Wu, C.; Zhao, D.; Xu, X.; Yang, J.; Feng, L.; Sun, Z.; Liu, L. Determining the Boundary and Probability of Surface Urban Heat Island Footprint Based on a Logistic Model. *Remote Sens.* **2019**, *11*, 1368–1388. [[CrossRef](#)]
33. Yang, J.; Huang, X. The 30 m Annual Land Cover Datasets and Its Dynamics in China from 1985 to 2022 [Data Set]. 2023. Available online: <https://zenodo.org/records/8176941> (accessed on 17 March 2024).
34. Sharma, M.; Bangotra, P.; Gautam, A.S.; Gautam, S. Sensitivity of normalized difference vegetation index (NDVI) to land surface temperature, soil moisture and precipitation over district Gautam Buddha Nagar, UP, India. *Stoch. Environ. Res. Risk Assess.* **2021**, *36*, 1779–1789. [[CrossRef](#)] [[PubMed](#)]
35. Chen, S.; Wang, T. Comparative Study on Defining Urban Heat Islands using Equidistant Method and Mean Standard Deviation Method. *J. Geo-Inf. Sci.* **2009**, *11*, 145–150. (In Chinese)
36. Almeida, C.R.d.; Teodoro, A.C.; Gonçalves, A. Study of the Urban Heat Island (UHI) Using Remote Sensing Data/Techniques: A Systematic Review. *Environments* **2021**, *8*, 105–144. [[CrossRef](#)]
37. Macarof, P.; Statescu, F. Comparaison of NDBI and NDVI as Indicators of Surface Urban Heat Island Effect in Landsat 8 Imagery: A Case Study of Iasi. *Present Environ. Sustain. Dev.* **2017**, *11*, 141–150. [[CrossRef](#)]
38. Zhou, L.; Zhang, K. Spatiotemporal Changes in Vegetation Coverage and Influencing Factors in Yan'an City from 2000 to 2020. *Bull. Soil Water Conserv.* **2023**, *43*, 356–365. (In Chinese) [[CrossRef](#)]
39. Du, G.; Sun, X.; Liu, Y.; Zheng, H.; Ma, R. Spatiotemporal Differentiation Characteristics of Ecological Retirement from Cultivated Land on the Loess Plateau. *J. Geo-Inf. Sci.* **2017**, *19*, 355–364. (In Chinese)
40. Yang, L.; Meng, T. Spatiotemporal Dynamics of Vegetation in Yan'an City over the Past 20 Years Based on MODIS Data. *West. Dev. (Res. Land Dev. Eng.)* **2020**, *5*, 64–70. (In Chinese)
41. Nie, T.; Dong, G.; Jiang, X.; Gu, J. Spatiotemporal Variation and Driving Forces of Vegetation Coverage in Yan'an Region. *Res. Soil Water Conserv.* **2021**, *28*, 340–346. (In Chinese) [[CrossRef](#)]
42. Wang, X.; Yang, J.; Lin, L.; Wei, X. Study on the Spatiotemporal Variation of Vegetation Coverage in Shaanxi Province Based on Sen+Mann-Kendall. *Agric. Technol.* **2023**, *43*, 62–66. (In Chinese) [[CrossRef](#)]
43. Xie, N. Dual Response of Vegetation Cover Change to Climate Change and Human Activities in Shaanxi Province (in Chinese). Master Thesis, Chang'an University, Xi'an, China, 8 April 2021.
44. Xie, S.; Mo, X.; Hu, S.; Chen, X. Response of Vegetation Greenness to Temperature and Precipitation in the Three-North Shelter Forest Engineering Area. *Geogr. Res.* **2020**, *39*, 152–165. (In Chinese)
45. Wang, H.; Liu, G.-h.; Li, Z.-s.; Ye, X.; Wang, M.; Gong, L. Driving force and changing trends of vegetation phenology in the Loess Plateau of China from 2000 to 2010. *J. Mt. Sci.* **2016**, *13*, 844–856. [[CrossRef](#)]
46. He, L.; Jia, Z.; Wang, Z. Land-use/cover spatial-temporal change characteristic in Yan'an region. *J. Nanjing For. Univ. (Nat. Sci. Ed.)* **2015**, *58*, 173–176.
47. Zhou, L.; Wang, P.; Cao, R. Analysis of soil erosion drivers and evaluation of ecological safety in Yan'an City, 2000–2020 (in Chinese). *J. Ecol. Rural Environ.* **2022**, *38*, 511–520.
48. Wang, Z.; Wu, J.; Bai, S.; Shi, F.; Yao, Z. Spatial and temporal changes of sloping cropland resources and its soil erosion effects in Yan'an City, China (in Chinese). *Res. Soil Water Conserv.* **2022**, *29*, 1–11.
49. Han, Z. Sensitivity evaluation of soil erosion in Yan'an city based on USLE (in Chinese). *Agric. Technol.* **2020**, *40*, 120–124.
50. Zaitunah, A.; Samsuri, S.; Silitonga, A.F.; Syaufina, L. Urban Greening Effect on Land Surface Temperature. *Sensors* **2022**, *22*, 4168. [[CrossRef](#)] [[PubMed](#)]
51. Zhao, H.; Tan, J.; Ren, Z.; Wang, Z. Spatiotemporal Characteristics of Urban Surface Temperature and Its Relationship with Landscape Metrics and Vegetation Cover in Rapid Urbanization Region. *Complexity* **2020**, *2020*, 7892362. [[CrossRef](#)]
52. Sun, Y.; Gao, C.; Li, J.; Li, W.; Ma, R. Examining urban thermal environment dynamics and relations to biophysical composition and configuration and socio-economic factors: A case study of the Shanghai metropolitan region. *Sustain. Cities Soc.* **2018**, *40*, 284–295. [[CrossRef](#)]
53. Manso, M.; Teotónio, I.; Silva, C.M.; Cruz, C.O. Green roof and green wall benefits and costs: A review of the quantitative evidence. *Renew. Sustain. Energy Rev.* **2021**, *13*, 110111. [[CrossRef](#)]
54. Cascone, S. Green Roof Design: State of the Art on Technology and Materials. *Sustainability* **2019**, *11*, 3020–3047. [[CrossRef](#)]
55. Santamouris, M.; Yun, G.Y. Recent development and research priorities on cool and super cool materials to mitigate urban heat island. *Renew. Energy* **2020**, *161*, 792–807. [[CrossRef](#)]
56. Feng, J.; Gao, K.; Santamouris, M.; Shah, K.W.; Ranzi, G. Dynamic impact of climate on the performance of daytime radiative cooling materials. *Sol. Energy Mater. Sol. Cells* **2020**, *208*, 110426. [[CrossRef](#)]

57. Estoque, R.C.; Murayama, Y.; Myint, S.W. Effects of landscape composition and pattern on land surface temperature: An urban heat island study in the megacities of Southeast Asia. *Sci. Total Environ.* **2017**, *577*, 349–359. [[CrossRef](#)] [[PubMed](#)]
58. Santos Nouri, A.; Costa, J.; Santamouris, M.; Matzarakis, A. Approaches to Outdoor Thermal Comfort Thresholds through Public Space Design: A Review. *Atmosphere* **2018**, *9*, 108. [[CrossRef](#)]
59. Miao, C.; Yu, S.; Hu, Y.; Zhang, H.; He, X.; Chen, W. Review of methods used to estimate the sky view factor in urban street canyons. *Build. Environ.* **2020**, *168*, 106497. [[CrossRef](#)]
60. Yang, G.; Yu, Z.; Jørgensen, G.; Vejre, H. How can urban blue-green space be planned for climate adaption in high-latitude cities? A seasonal perspective. *Sustain. Cities Soc.* **2020**, *53*, 101932. [[CrossRef](#)]
61. Lin, J.; Qiu, S.; Tan, X.; Zhuang, Y. Measuring the relationship between morphological spatial pattern of green space and urban heat island using machine learning methods. *Build. Environ.* **2023**, *228*, 109910. [[CrossRef](#)]
62. Liu, W.; Zhao, H.; Sun, S.; Xu, X.; Huang, T.; Zhu, J. Green Space Cooling Effect and Contribution to Mitigate Heat Island Effect of Surrounding Communities in Beijing Metropolitan Area. *Front. Public Health* **2022**, *10*, 870403. [[CrossRef](#)]

Disclaimer/Publisher’s Note: The statements, opinions and data contained in all publications are solely those of the individual author(s) and contributor(s) and not of MDPI and/or the editor(s). MDPI and/or the editor(s) disclaim responsibility for any injury to people or property resulting from any ideas, methods, instructions or products referred to in the content.